Supporting Information

Heterogeneous structure engineering and optimizing electronic band structure of $VO_2(B)/V_3O_5$ cathode: Toward low-cost, long life span and green aqueous ammonium ion battery

Miaomiao Liang[a], Maosen Hu[a], Yiwei Si[a], Rui Xue[a], Yongxia Kang[a], Hemeng Zhang[a], Haiyang Wang[b,c,*], Zongcheng Miao[b,c,*], Chong Fu[a,*]

[a]School of Materials Science and Engineering, Xi'an Key Laboratory of Textile CompositesKey Laboratory of Functional Textile Material and Product, Ministry of Education, Xi'an Key Laboratory of Textile Composites, Xi'an Polytechnic University, Xi'an, 710048, China

[b]Technological Institute of Materials & Energy Science (TIMES), Key Laboratory of Liquid Crystal Polymers based Flexible Display Technology in National Petroleum and Chemical Industry, Xi'an Key Laboratory of Advanced Photo-electronics Materials and Energy Conversion Device, School of Electronic Information, Xijing University, Xi'an, 710123, P.R. China

[c]School of Artificial Intelligence, Optics and Electronics (iOPEN), Northwestern Polytechnical University, Xi'an, 710072, Shaanxi, China

E-mail addresses: why0224@126.com; miaozongcheng@nwpu.edu.cn; fuchong69@163.com

Fig. S1 The survey spectrum of (a) $VO_2(B)/V_3O_5$, (b)$Fe_{0.05}VO_2(B)/V_3O_5$, (c) $Fe_{0.1}VO_2(B)/V_3O_5$, (d) $Fe_{0.15}VO_2(B)/V_3O_5$

Sample Name	Mass m_0 (g)	Constant Volume V_0 (mL)	Test Element	Concentration of tested element in solution C_0 (mg/L)	Dilution factor f	Element concentration in original decomposition reagent C_1 (mg/L)	Element Content C_x (mg/kg)	Element Content W %	Fe:V %
$VO_2(B)/V_3O_5$	0.0426	50	Fe	0.172	1	0.172	202.1	0.02%	0.05%
			V	317.268	1	317.268	372730.3	37.27%	
$Fe_{0.05}VO_2(B)/V_3O_5$	0.03971	50	Fe	6.213	1	6.213	7823.0	0.78%	2.07%
			V	299.731	1	299.731	377399.9	37.74%	
$Fe_{0.1}VO_2(B)/V_3O_5$	0.03682	50	Fe	13.877	1	13.877	18844.4	1.88%	4.05%
			V	286.534	1	286.534	389101.0	38.91%	
$Fe_{0.15}VO_2(B)/V_3O_5$	0.041	50	Fe	23.279	1	23.279	28389.0	2.84%	7.65%
			V	304.159	1	304.159	370925.6	37.09%	

Table S1 The specific ICP results of $VO_2(B)/V_3O_5$, $Fe_{0.05}VO_2(B)/V_3O_5$, $Fe_{0.1}VO_2(B)/V_3O_5$, $Fe_{0.15}VO_2(B)/V_3O_5$ sample

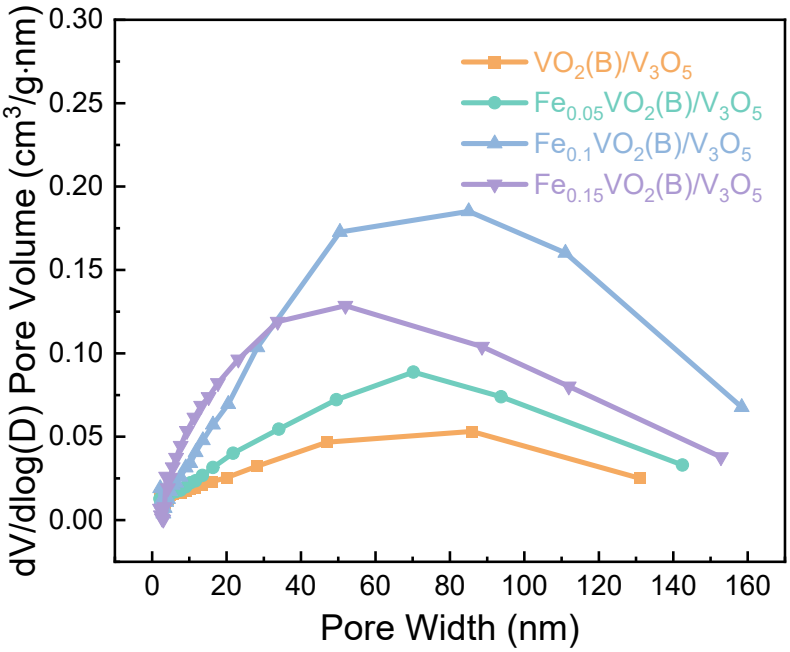

Fig. S2 The BJH pore size distribution of samples.

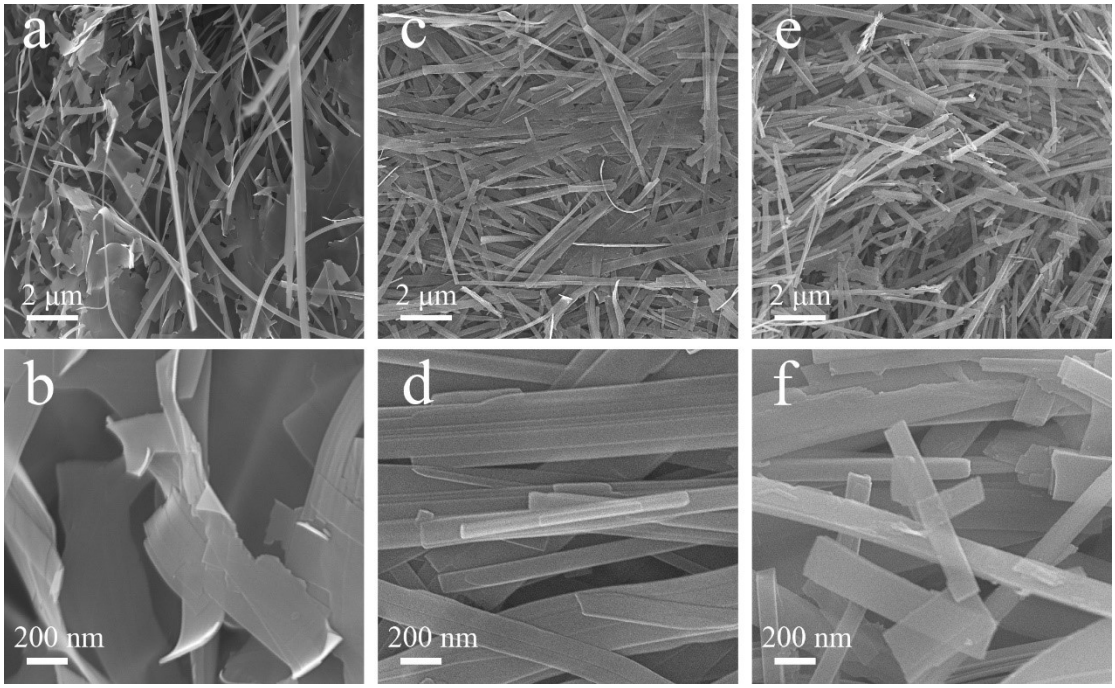

Fig. S3 SEM images of (a), (b) $VO_2(B)/V_3O_5$, (c), (d) $Fe_{0.05}VO_2(B)/V_3O_5$, (e), (f) $Fe_{0.15}VO_2(B)/V_3O_5$

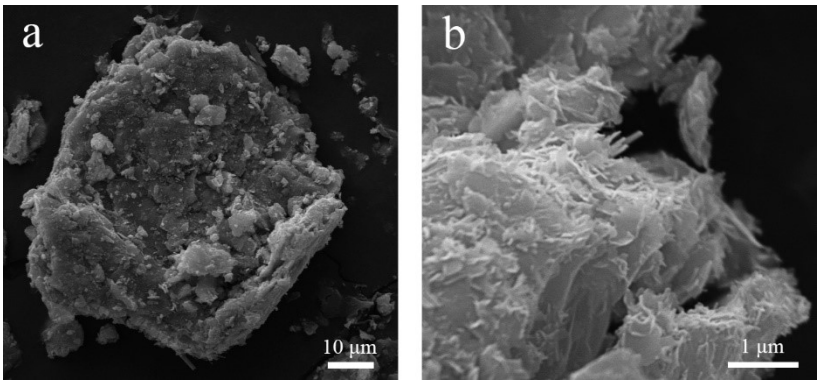

Fig. S4 SEM images of $Fe_{0.1}VO_2(B)/V_3O_5$ with no addition of PEG-4000

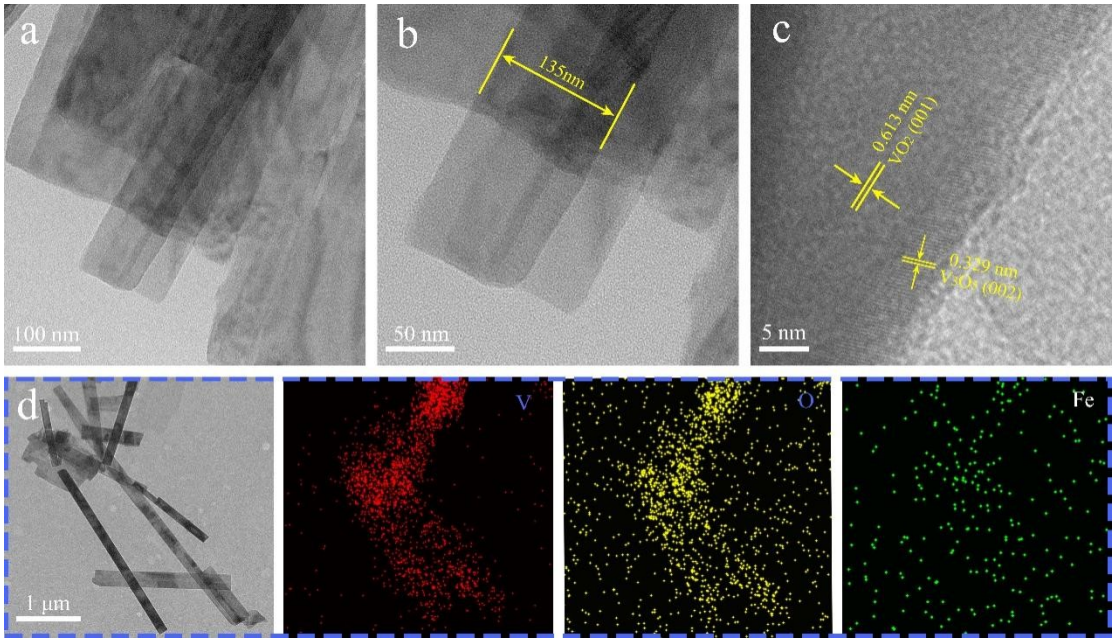

Fig. S5 (a), (b) TEM and (c) HRTEM images of $VO_2(B)/V_3O_5$. (d) Element mapping of V, Fe, O in $VO_2(B)/V_3O_5$

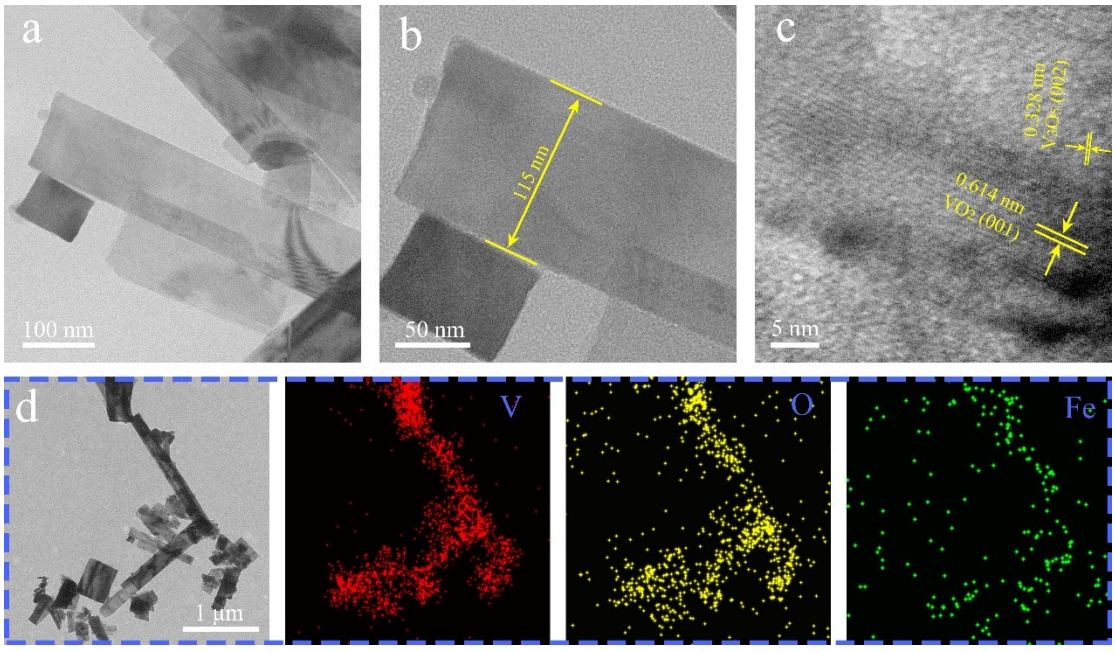

Fig. S6 (a), (b) TEM and (c) HRTEM images of $Fe_{0.05}VO_2(B)/V_3O_5$. (d) Element mapping of V, Fe, O in Fe $Fe_{0.05}VO_2(B)/V_3O_5$

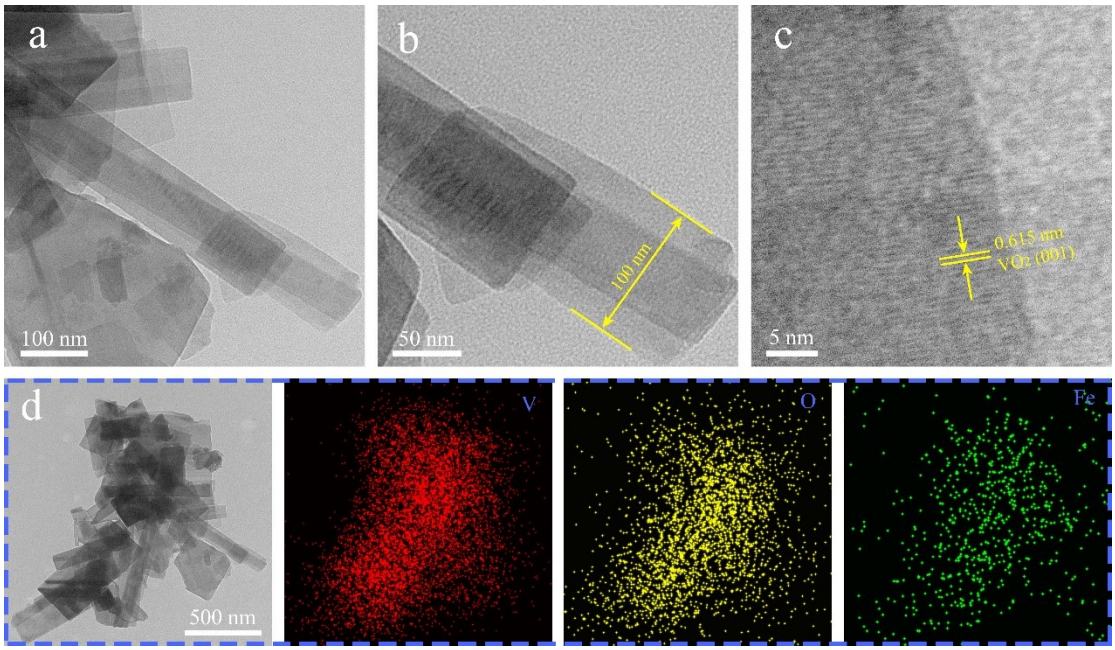

Fig. S7 (a), (b) TEM and (c) HRTEM images of $Fe_{0.15}VO_2(B)/V_3O_5$. (d) Element mapping of V, Fe, O in $Fe_{0.15}VO_2(B)/V_3O_5$

Fig. S8 (a) CVs at varied scan rate and (b) GCDs at different current density of $VO_2(B)/V_3O_5$

Fig. S9 (a) CVs at varied scan rate and (b) GCDs at different current density of $Fe_{0.05}VO_2(B)/V_3O_5$

Fig. S10 (a) CVs at varied scan rate and (b) GCDs at different current density of $Fe_{0.1}VO_2(B)/V_3O_5$

Fig. S11 (a) CVs at varied scan rate and (b) GCDs at different current density of $Fe_{0.15}VO_2(B)/V_3O_5$

Fig. S12 Equivalent circuit of (a) $VO_2(B)/V_3O_5$, (b) $Fe_{0.05}VO_2(B)/V_3O_5$, (c) $Fe_{0.1}VO_2(B)/V_3O_5$, (d) $Fe_{0.15}VO_2(B)/V_3O_5$ electrode, respectively

Fig. S13 GITT of (a) $VO_2(B)/V_3O_5$, (b) $Fe_{0.05}VO_2(B)/V_3O_5$, (c) $Fe_{0.15}VO_2(B)/V_3O_5$, respectively

Fig. S14 Diffusion contribution to charge storage of (a) $VO_2(B)/V_3O_5$, (b) $Fe_{0.05}VO_2(B)/V_3O_5$, (c) $Fe_{0.1}VO_2(B)/V_3O_5$, (d) $Fe_{0.15}VO_2(B)/V_3O_5$ electrode, respectively.

Sample Name	Mass m_0 (mL)	Constant Volume V_0 (mL)	Test Element	Concentration of tested element in solution C_0 (mg/L)	Dilution factor f	Element concentration in original decomposition reagent C_1 (mg/L)	Element Content C_x (mg/L)
$Fe_{0.1}VO_2(B)/V_3O_5$	5	50	Fe	0.146	1	0.146	1.46
			V	2.785	1	2.785	27.85

Table S2 The specific ICP results of $Fe_{0.1}VO_2(B)/V_3O_5$ sample after cycle

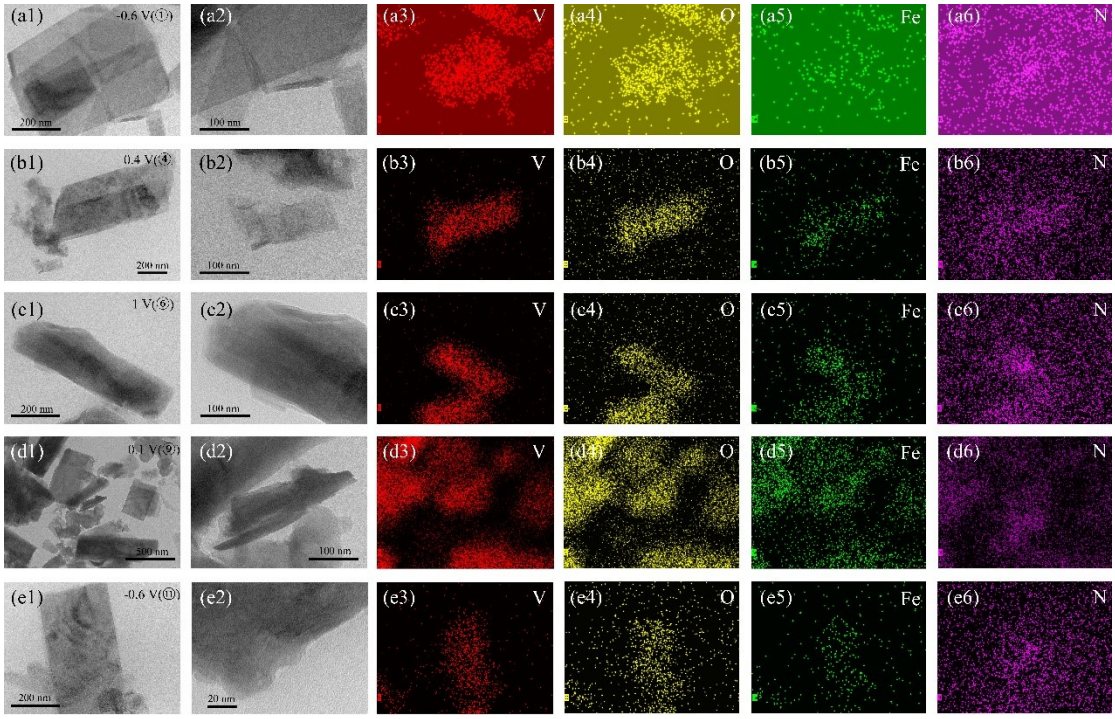

Fig. S15 TEM images and EDS of samples at specific charge/discharge voltage

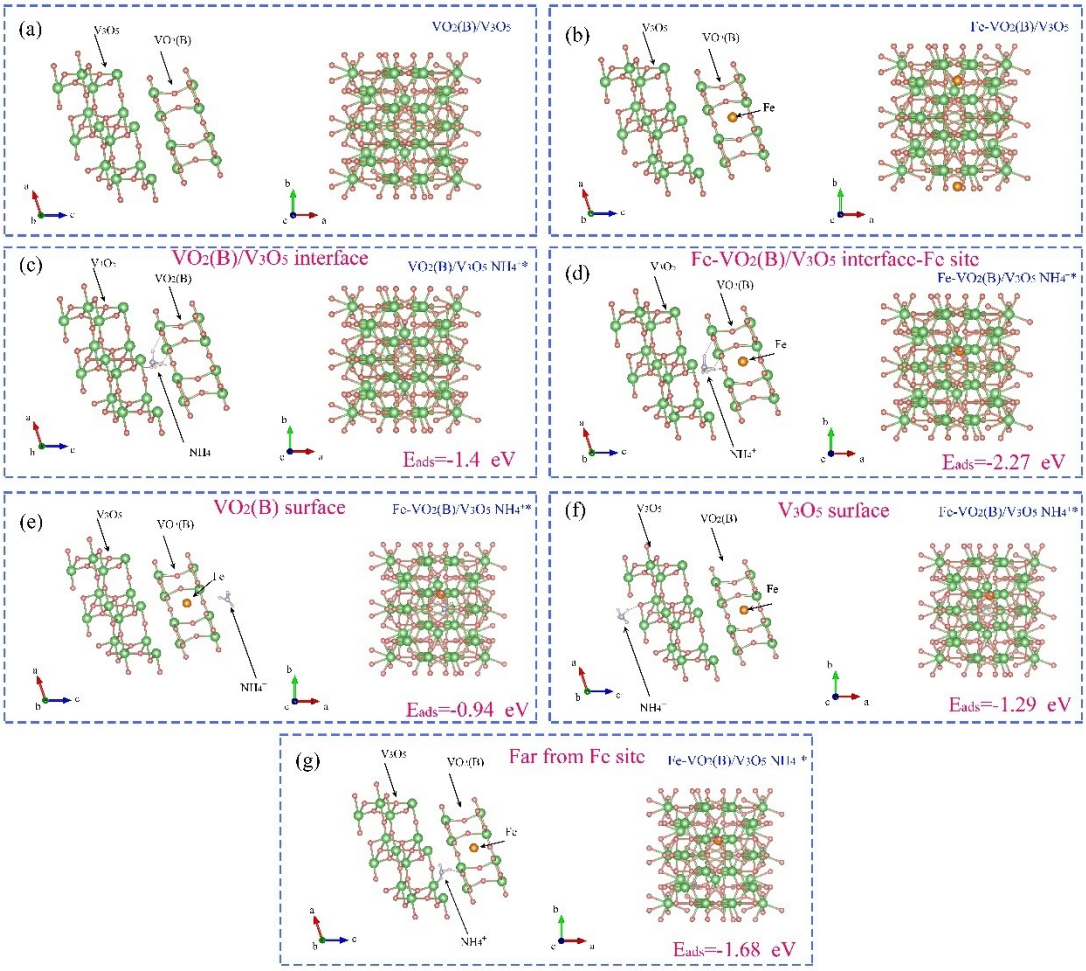

Fig. S16 Side-view and top-view schematic sketch of bond states for (a) $VO_2(B)/V_3O_5$, (b) Fe-$VO_2(B)/V_3O_5$ and insertion of NH_4^+ into (c) $VO_2(B)/V_3O_5$ interface, (d) Fe site of Fe-$VO_2(B)/V_3O_5$ interface, (e) $VO_2(B)$ surface, (f) V_3O_5 surface, and (g) NH_4^+ adsorption at far from Fe site of Fe-$VO_2(B)/V_3O_5$

Fig. S17 The electrochemical performance of PTCDI in three-electrode system. (a) CV curves at different scan rates. (b) GCD profiles. (c) Rate performance. (d) EIS plot.

Fig. S18 CV profiles (a) at different scan rate and (b) different voltage window of $VO_2(B)/V_3O_5$//

PTCDI

Fig. S19 CV profiles (a) at different scan rate and (b) different voltage window of $Fe_{0.05}VO_2(B)/V_3O_5$//

PTCDI

Fig. S20 CV profiles (a) at different scan rate and (b) different voltage window of $Fe_{0.1}VO_2(B)/V_3O_5$//

PTCDI

Fig. S21 CV profiles (a) at different scan rate and (b) different voltage window of $Fe_{0.15}VO_2(B)/V_3O_5$// PTCDI

Fig. S22 Equivalent circuit of (a) $VO_2(B)/V_3O_5$//PTCDI, (b) $Fe_{0.05}VO_2(B)/V_3O_5$//PTCDI, (c) $Fe_{0.1}VO_2(B)/V_3O_5$//PTCDI, (d) $Fe_{0.15}VO_2(B)/V_3O_5$//PTCDI electrode, respectively